Macromolecules

COMMUNICATION TO THE EDITOR

pubs.acs.org/Macromolecules

Highly Ordered Poly(3-hexylthiophene) Rod Polymers via Block Copolymer Self-Assembly

Su Yeon Choi,[†] Jea Uk Lee,[‡] Jin Wook Lee,[†] Sle Lee,[†] Yun Jeong Song,[‡] Won Ho Jo,[*,‡] and Seung Hyun Kim[*,†]

[†]Division of Nano-Systems Engineering, Inha University, Incheon 402-751, Republic of Korea

[‡]Department of Materials Science and Engineering, Seoul National University, Seoul 151-742, Republic of Korea

Supporting Information

Over the past decade, remarkable progress for full utilization of conducting polymers in various electronic and optoelectronic applications has been achieved with the improvement of device performance based on advance in designing new conducting polymers and better understanding of device physics.[1−3] At the same time, it has been demonstrated that the structure on the nanometer and micrometer scales as well as the electronic properties inherent to conducting polymers are key in determining properties and ultimate device performance.[4−9] Among several strategies, the self-assembly of block copolymer (BCP) can offer effective means to control the nanoscale morphology because they, consisting of two or more chemically different macromolecules that are connected covalently, can self-assemble to produce well-defined structure on the molecular scale.[10] Moreover, methodologies recently developed for manipulating self-assembly raise our expectations for utilization of BCP containing conducting polymers.[11−20] Organic photovoltaic (OPV) cells and field-effect transistors (FFTs) are the applications that can receive the greatest benefit from such BCP self-assembly and have intensively been investigated so far.[13,17] However, although a number of works on conducting BCPs have been published and their number is ever-increasing, their applications are very limited due to poor performance. Such poor performance mainly results from difficulty in controlling the self-assembly of conducting BCPs due to inherent chain rigidity of conducting polymers. Basically, the phase behavior of conducting BCPs is much different from that of conventional BCPs with flexible chains. In this work, by using BCPs containing poly(3-hexylthiophene) (P3HT) as a conducting polymer, well-controlled, well-ordered nanostructure over large area which have never been observed before was produced for better performance.

BCPs containing P3HT were synthesized through the use of controlled Grignard metathesis (GRIM) polymerization method and subsequent atom transfer radical polymerization (ATRP) that was previously developed by McCullough and co-workers.[21,22] P3HT macroinitiator synthesized in this work exhibited 98% regioregulaity and narrow molecular weight distribution with M_w/M_n = 1.3 and was used for copolymerization of methyl methacrylate (MMA) to produce rod−coil P3HT-*b*-PMMA BCPs with different compositions. Figure 1 shows the surface morphologies of films of P3HT-*b*-PMMA copolymer with P3HT of 10 kg/mol and PMMA of 15 kg/mol cast on silicon wafer. The film thickness was in the range of 80−100 nm, and the solvent was evaporated very slowly under saturated solvent vapor. As-cast copolymer film, as shown in

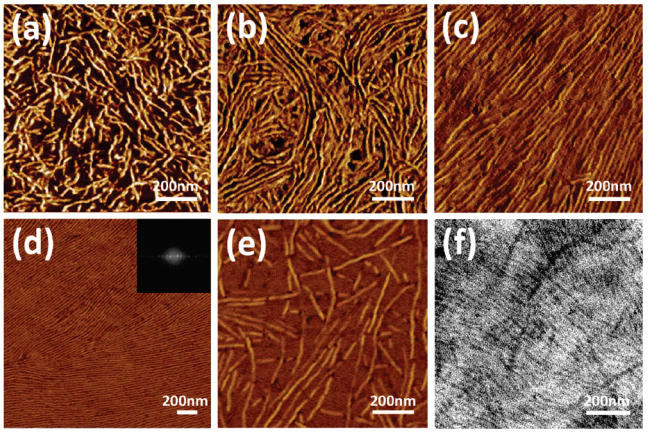

Figure 1. AFM images of (a) as-cast P3HT-*b*-PMMA film, (b) solvent-annealed P3HT-*b*-PMMA film, (c) as-cast P3HT-*b*-PMMA/P3HT (9/1) blend film, (d) as-cast P3HT-*b*-PMMA/PMMA (9/1) blend film, and (e) as-cast P3HT-*b*-PMMA/PMMA (7/3) blend film and TEM micrograph of (f) P3HT-*b*-PMMA/PMMA (9/1) blend film after PMMA removal.

Figure 1a, exhibits the fibril-like structure that is typical rod-like P3HT morphology due to its crystallization. However, the fibrils are randomly oriented, and their degree of order is poor. Solvent-annealing for 12 h slightly improves fibril packing with its length increased (Figure 1b), but its effects are not so dominant as in the case of conventional coil−coil BCPs.[23] On the other hand, when small amounts of homopolymers were added to BCP solution, the lateral order of microphase-separated domains significantly improved, as shown Figure 1c,d. Especially, in the PMMA case, highly ordered nanofibril structure was produced, and the fibril length was extended over tens of micrometers. Fourier transform of the image in the inset exhibits the perfection of lamellar order. It should be noted that such well-ordered nanostructure was produced for as-cast films without additional annealing process. In order to clearly show long-range lateral order, large-area AFM image was additionally provided in Figure S1 of the Supporting Information, where defects marked by the different colors of circles were used to connect a series of AFM images. With the content further increasing, however, added homopolymers were separated from BCP

Received: October 24, 2010
Revised: February 7, 2011
Published: March 03, 2011

ACS Publications © 2011 American Chemical Society

domains to generate their own domains via macrophase separation (Figure 1e). The composition effects with lower amount of homopolymers can be observed in the Figure S2 in the Supporting Information. Even only at 3 wt %, the order of P3HT blocks improved significantly, but the order is near perfection at 10 wt % homopolymers added. The prerequisites for achieving long-range ordering of BCPs are sufficient chain mobility and high χ value.[23] In our work, BCP films were generated under fully saturated solvent vapor, which would provide copolymer chains with sufficient mobility. Another prerequisite would be met by blending BCPs with homopolymers. Previous studies have shown that depending on the molecular weight of homopolymer relative to that of corresponding block, three different distributions of homopolymers take place: homogeneous distribution within the domains of corresponding blocks, segregation to the central region of block domains, and macrophase separation from BCP nanostructure.[24,25] Furthermore, in thin films, it has been reported that addition of homopolymers tends to reorient the microdomains from parallel to perpendicular and enhance the degree of order.[26,27] In order to understand all these phenomena, the enthalpic contributions in addition to entropic contributions should be properly considered from blending with homopolymers. Indeed, the intermolecular interaction between homopolymers and corresponding blocks was found to increase the incompatibility between components to induce the orientation change and enhance the order.[26,27] The increase in incompatibility between the components of BCP due to the presence of additives such as salts, surfactants, or liquid crystals has also been reported in other cases.[28,29] In our case, added homopolymers are expected to play a similar role in improving the degree of order of BCP nanostructure. The effects are found to be more prominent for PMMA homopolymer than for P3HT homopolymer. It should be noted that PMMA has lower molecular weight than the PMMA block while P3HT is much larger than the P3HT block. However, not all BCPs with different compositions exhibit long-range order, but highly ordered nanostructure was obtained over limited composition range. All parameters such as block composition, molecular weight, interaction between components, etc., appear to work together in determining the nanostructure of BCPs.

PMMA can be easily degraded and removed on exposure to deep UV lights, which is one of the reasons why PMMA has been adopted as a coil block in this work. Nanoporous template generated by selective removal of sacrificial block from BCP film can be used to introduce new functional materials into the holes. If the electron-acceptor materials will be able to be incorporated after PMMA removal, ideal heterojuction nanostructure may be formed for OPV cells by combination with highly ordered P3HT phases. Figure 1f displays the TEM image for BCP film after PMMA removal. BCP film was observed to maintain highly ordered nanostructure after PMMA degradation. Similar results have been reported in the previous works,[30−32] where selective removal of one component produced nanoporous P3HT films. Hillmyer's group synthesized P3HT-*b*-PLA and selectively removed PLA,[30] Hawker's group used P3HT-*g*-PS graft copolymer with cleavable junction to remove PS domains,[31] and Hiashihara et al. used the ionic interaction between P3HT-NH_2 and PS-SO_3H to synthesize the BCP and produce the P3HT nanoporous film by etching out PS-SO_3H domains.[32] However, their nanoporous structures were initially ill-defined, ill-ordered, and/or collapsed during formation of nanoporous films. In terms of applications of our BCP, there still exist problems to be overcome such as effective infiltration and thereafter formation of robust

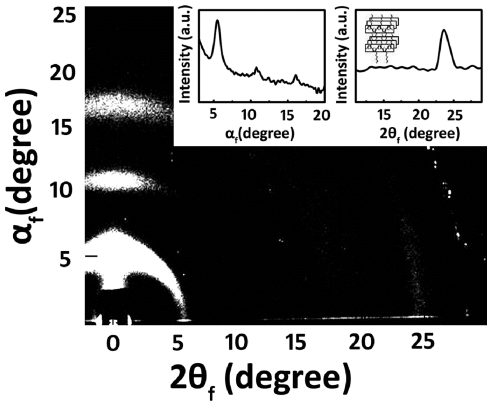

Figure 2. GIWAXD pattern of P3HT-*b*-PMMA/PMMA (9/1) blend film. The inset includes the out-of-plane and in-plane profiles extracted from GIWAXD pattern, respectively.

interface with existing P3HT phases. Nevertheless, in our work, self-assembled nanostructure with high degree of order in BCP films containing P3HT was obtained with unprecedented success, making one step further toward real applications of conducting BCPs such as FET and OPV where charge-transporting properties are decisive of determining their performance.

The orientation and packing of P3HT chains are also important factors to affect their charge-transporting properties and ultimate performance. Grazing-incidence X-ray wide-angle diffraction (GIWAXD) experiments were conducted to explore the molecular ordering of P3HT chains in film, and the results are included in Figure 2 where P3HT-*b*-PMMA/PMMA (9/1) film was measured at incident angle $\alpha_i = 0.18°$. Two insets correspond to the out-of-plane profile scanned along the α_f direction at $2\theta = 0°$ and in-plane scan extracted along the 2θ direction at $\alpha_f = 0.18°$ from GIWAXD pattern, respectively. In the out-of-plane profile, strong (100) reflections due to lamellar stacking oriented parallel to the substrate are evident, while a (010) reflection due to $\pi-\pi$ interchain stacking of P3HT is observed in in-plane scan. These observations indicate that P3HT blocks still have edge-on orientation in the BCP geometry as in the case of homopolymer chain where the hexyl side chains of the P3HT blocks are oriented normal to the silicon wafer and the intermolecular $\pi-\pi$ stacking between thiophene rings is parallel to the substrate. Similar patterns were observed for BCP films without added homopolymer, implying that the orientation and packing of P3HT blocks that are connected to flexible PMMA chains are the same as those of homopolymer chains. Therefore, P3HT blocks in BCP domains are expected to have the properties and performance with the same level as P3HT homopolymers do. Considering highly ordered nanostructure that P3HT-containing BCPs exhibit in thin film geometry, these results are quite promising for their potential applications.

Figure 3a shows UV−vis absorption spectra of P3HT-containing BCP films that can provide another insight into the molecular ordering of P3HT blocks such as conjugation length and intrachain/interchain. BCP film without added homopolymers exhibits the vibronic features characteristic of regioregular P3HT homopolymer chains with highly ordered lamellae, indicating the P3HT backbones in BCP are highly ordered such as in homopolymer. Blend film with PMMA homopolymers of 10 wt % exhibits similar or slightly improved ordering of P3HT blocks. However, as the content of PMMA added increases up to 30 wt %, the absorption shoulder at 610 nm is weakened

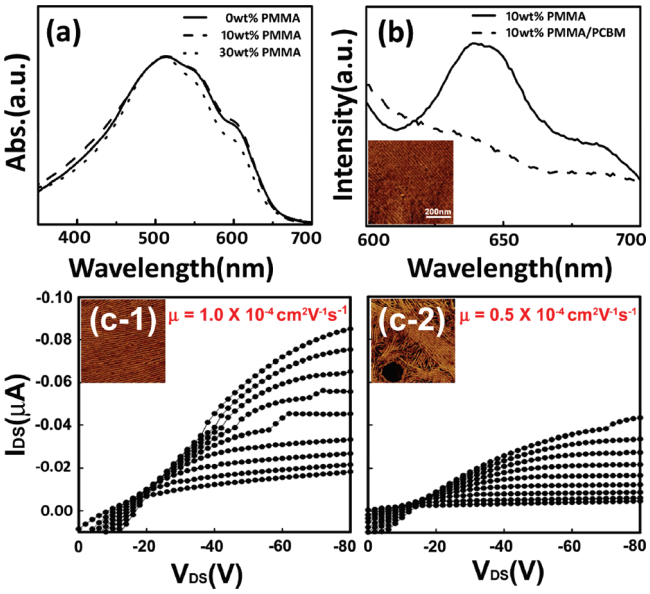

Figure 3. (a) UV−vis absorption of P3HT-*b*-PMMA and its blends with PMMA homopolymers. (b) PL spectra of P3HT-*b*-PMMA/PMMA (9/1) (—) and its mixture with PCBM (---). (c) Current−voltage curves of FET devices consisting of P3HT-*b*-PMMA/PMMA (9/1) blend film at different gate voltages (of 0, −10, 20, −30, −40, −50, −60, −70, and −80 V from the bottom). The AFM image of active layer and field-effect motility of device are inserted in each graph.

significantly, indicating that the interchain order of P3HT was disturbed by excess of added homopolymers.

The potential for OPV application of conducting BCP used in this work was investigated through blending with [6,6]-phenyl-C61-butyric acid methyl ester (PCBM, Nano-C) because PCBM can be combined with P3HT to produce bulk heterojunction solar cells. For the purpose, photoluminescence was measured for mixtures of P3HT-*b*-PMMA/PMMA (9/1) and PCBM, as shown in Figure 3b. Here, PCBM was added to P3HT-*b*-PMMA/PMMA blend without removal of PMMA but is still expected to be preferentially located along the PMMA microdomains due to strong repulsion with P3HT chains. Addition of PCBM has little effect on the ordering behavior of BCP blend; still highly ordered nanostructure was observed. However, compared to that without PCBM, the photoluminescence of P3HT is significantly quenched after addition of PCBM, which means that the charge transfer across the interface takes place. Such result indicates that PCBM molecules are well distributed along the nanostructure, and such highly ordered nanostructure generated by BCP self-assembly can provide a platform for OPV although high energy conversion efficiency cannot be expected here due to the presence of large amount of dielectric PMMA.

Another potential application of our block copolymer systems was probed to measure the field-effect characteristics. For the purpose, the field-effect transistors were fabricated in bottom-gate configuration on heavily doped n-type Si substrate as the gate electrode and a thermally grown 300 nm silicone dioxide as a dielectric layer. The measured results were added in Figure 3c, together with the average field-effect mobility of the transistors calculated from the slope of a line drawn through the linear plot of square-root drain current ($I_{DS}^{1/2}$) versus gate voltage (V_G) in the saturation regime. As in the case of OPV application, the presence of large amount of PMMA blocks and homopolymers still limit their real applications and do not exhibit so excellent properties as expected from highly ordered nanostructure of block copolymer films including P3HT. Moreover, our experimental conditions for measurements of field-effect mobility were not optimized perfectly; indeed, measured mobility is not so high as that presented in ref 13. Nonetheless, relatively high field-effect mobility was obtained for our BCP films, and that for film with highly ordered structure (Figure 3c-1) was higher twice than that with less-ordered structure (Figure 3c-2). The order in films was here controlled to various degrees by adjusting the evaporation rate of solvent on casting the film. The field-effect mobility for films with poor order could hardly be measured in this work.

In conclusion, highly ordered nanostructure of conducting polymers through BCP self-assembly was successfully produced, which, combined with high degree of order of conducting polymer chains in their domains, can provide great opportunity for electronic and optoelectrical applications with much improved performance.

■ ASSOCIATED CONTENT

Supporting Information. Experimental details on film formation of block copolymer and its blends with homopolymer and measurements of field-effect characteristics and AFM images showing the order over large area and blend composition effects. The material is available free of charge via the Internet at http://pubs.acs.org.

■ AUTHOR INFORMATION

Corresponding Author

*Ph +82-32-860-7493, Fax +82-32-873-0181, e-mail shk@inha.ac.kr (S.H.K.); Ph +82-2-880-7192, Fax +82-2-885-1748, e-mail whjpoly@snu.ac.kr (W.H.J.).

■ ACKNOWLEDGMENT

This work was financially supported through the Global Research Laboratory (GRL) program and by the National Research Foundation of Korea (NRF) grant (No. 2010-0015541) funded by the Ministry of Education, Science and Technology (MEST). Experiments at PLS were supported in part by MEST and POSTECH.

■ REFERENCES

(1) Blouin, N.; Michaud, A.; Gendron, D.; Wakim, S.; Blair, E.; Neagu-Plesu, R.; Belletete, M.; Durocher, G.; Tao, Y.; Leclerc, M. *J. Am. Chem. Soc.* **2008**, *130*, 732–742.

(2) Li, Q. Q.; Zou, J. H.; Chen, J. W.; Liu, Z. J.; Qin, J. G.; Li, Z.; Cao, Y. *J. Phys. Chem. B* **2009**, *113*, 5816–5822.

(3) Park, S. H.; Roy, A.; Beaupre, S.; Cho, S.; Coates, N.; Moon, J. S.; Moses, D.; Leclerc, M.; Lee, K.; Heeger, A. J. *Nature Photonics* **2009**, *3*, 297–U5.

(4) Barrau, S.; Andersson, V.; Zhang, F. L.; Masich, S.; Bijleveld, J.; Andersson, M. R.; Inganas, O. *Macromolecules* **2009**, *42*, 4646–4650.

(5) Blom, P. W. M.; Mihailetchi, V. D.; Koster, L. J. A.; Markov, D. E. *Adv. Mater.* **2007**, *19*, 1551–1566.

(6) Muccini, M. *Nature Mater.* **2006**, *5*, 605–613.

(7) Verilhac, J. M.; LeBlevennec, G.; Djurado, D.; Rieutord, F.; Chouiki, M.; Travers, J. P.; Pron, A. *Synth. Met.* **2006**, *156*, 815–823.

(8) Yang, X. N.; Loos, J.; Veenstra, S. C.; Verhees, W. J. H.; Wienk, M. M.; Kroon, J. M.; Michels, M. A. J.; Janssen, R. A. J. *Nano Lett.* **2005**, *5*, 579–583.

(9) Zhang, Y.; Tajima, K.; Hashimoto, K. *Macromolecules* **2009**, *42*, 7008–7015.
(10) Kim, H. C.; Park, S. M.; Hinsberg, W. D. *Chem. Rev.* **2010**, *110*, 146–177.
(11) Botiz, I.; Martinson, A. B. F.; Darling, S. B. *Langmuir* **2010**, *26*, 8756–8761.
(12) de Cuendias, A.; Le Hellaye, M.; Lecommandoux, B.; Cloutet, E.; Cramail, H. *J. Mater. Chem.* **2005**, *15*, 3264–3267.
(13) Sauvé, G.; McCullough, R. D. *Adv. Mater.* **2007**, *19*, 1822–1825.
(14) Iovu, M. C.; Zhang, R.; Cooper, J. R.; Smilgies, D. M.; Javier, A. E.; Sheina, E. E.; Kowalewski, T.; McCullough, R. D. *Macromol. Rapid Commun.* **2007**, *28*, 1816–1824.
(15) Kim, D. H.; Lee, B. L.; Moon, H.; Kang, H. M.; Jeong, E. J.; Park, J. I.; Han, K. M.; Lee, S.; Yoo, B. W.; Koo, B. W.; Kim, J. Y.; Lee, W. H.; Cho, K.; Becerril, H. A.; Bao, Z. *J. Am. Chem. Soc.* **2009**, *131*, 6124–6132.
(16) Richard, F.; Brochon, C.; Leclerc, N.; Eckhardt, D.; Heiser, T.; Hadziioannou, G. *Macromol. Rapid Commun.* **2008**, *29*, 885–891.
(17) Sary, N.; Richard, F.; Brochon, C.; Leclerc, N.; Leveque, P.; Audinot, J.-N.; Berson, S.; Heiser, T.; Hadziioannou, G.; Mezzenga, R. *Adv. Mater.* **2010**, *22*, 763–768.
(18) Sommer, M.; Lang, A. S.; Thelakkat, M. *Angew. Chem., Int. Ed.* **2008**, *47*, 7901–7904.
(19) Zhang, Q. L.; Cirpan, A.; Russell, T. P.; Emrick, T. *Macromolecules* **2009**, *42*, 1079–1082.
(20) Yang, G. Z.; Chen, X. L.; Wang, L. M.; Shi, J. G.; Li, C. Z.; Liu, T. X. *Polym. Adv. Technol.* **2009**, *20*, 104–110.
(21) Iovu, M. C.; Jeffries-El, M.; Sheina, E. E.; Cooper, J. R.; McCullough, R. D. *Polymer* **2005**, *46*, 8582–8586.
(22) Lee, J. U.; Cirpan, A.; Emrick, T.; Russell, T. P.; Jo, W. H. *J. Mater. Chem.* **2009**, *19*, 1483–1489.
(23) Kim, S. H.; Misner, M. J.; Xu, T.; Kimura, M.; Russell, T. P. *Adv. Mater.* **2004**, *16*, 226–231.
(24) Torikai, N.; Takabayashi, N.; Nosda, I.; Koizumi, S.; Morii, Y.; Matsushita, Y. *Macromolecules* **1997**, *30*, 5698–5703.
(25) Matsen, M. W. *Macromolecules* **2003**, *36*, 9647–9657.
(26) Ahn, D.; Sancaktar, E. *Adv. Funct. Mater.* **2006**, *16*, 1950–1958.
(27) Jeong, U.; Ryu, D.; Kho, D.; Kim, J.; Goldbach, J.; Kim, D.; Russell, T. *Adv. Mater.* **2004**, *16*, 533–536.
(28) Kim, S. H.; Misner, M. J.; Yang, L.; Gang, O.; Ocko, B. M.; Russell, T. P. *Macromolecules* **2006**, *39*, 8473–8479.
(29) Lee, C.; Kim, S. H.; Russell, T. P. *Macromol. Rapid Commun.* **2009**, *30*, 1674–1678.
(30) Boudouris, B. W.; Frisbie, C. D.; Hillmyer, M. A. *Macromolecules* **2008**, *41*, 67–75.
(31) Sivanandan, K.; Chatterjee, T.; Treat, N.; Kramer, E. J.; Hawker, C. J. *Macromolecules* **2010**, *43*, 233–241.
(32) Takahashi, A.; Rho, Y.; Higashihara, T.; Ahn, B.; Ree, M.; Ueda, M. *Macromolecules* **2010**, *43*, 4843–4852.